Planet. Space Sci., Vol. 41, No. 3, pp. 173–181, 1993
Printed in Great Britain.

0032–0633/93 $6.00+0.00
© 1993 Pergamon Press Ltd

Coherent backscatter and the opposition effect for E-type asteroids

M. I. Mishchenko* and J. M. Dlugach

The Main Astronomical Observatory, Ukrainian Academy of Sciences, 252127 Kiev, Ukraine

Received 17 June, 1992; revised 3 November, 1992; accepted 29 December, 1992

Abstract. Recently, Harris *et al.* (*Icarus* **81,** 365–374, 1989) have observed a strong and unusually narrow (HWHM $\simeq 0.8°$ in the yellow) opposition effect for high-albedo asteroids 44 Nysa and 64 Angelina. In this paper, we apply the theory of coherent backscattering of light from discrete random media to interpret this remarkable opposition brightening. It is shown that coherent backscattering of sunlight from a regolithic layer composed of submicrometer-sized grains with an index of refraction close to that of the mineral enstatite can be a reasonable explanation of the observed opposition effect.

1. Introduction

The shadowing models by Hapke (1986) and Lumme and Bowell (1981) have been widely used to interpret the opposition brightening exhibited by many atmosphereless solar system bodies. Nevertheless, as was noted by Buratti (1991), more extensive laboratory measurements of the bidirectional reflectance properties of various materials are necessary to understand how physically realistic it is to compare astronomical and spacecraft observations with these models. Moreover, there are situations in which the formal fit of theoretical curves to observational data becomes impossible or physically meaningless. Indeed, the opposition effect observed for Saturn's A- and B-rings (Franklin and Cook, 1965) and icy outer planet satellites (Brown and Cruikshank, 1983; Goguen *et al.*, 1989; Domingue *et al.*, 1991; Thompson and Lockwood, 1992) at visible and near-infrared wavelengths has the angular semi-width of only a few tenths of degree. Such a narrowness of the opposition effect, if explained on the basis of the shadowing models, implies an unrealistically low volume density of the upper, optically active regolithic layer. Recently, Harris *et al.* (1989) (see also Lagerkvist *et al.*, 1992) have measured a similar opposition effect for high-albedo asteroids 44 Nysa and 64 Angelina (Fig. 1) and concluded that, apparently, the well-known shadowing mechanism cannot reproduce satisfactorily this unusual opposition brightening.

Kuga and Ishimaru (1984) and O'Donnell and Mendez (1987) were the first to mention the opposition effect of the lunar surface near full moon in the context of the so-called coherent backscattering mechanism. Later, in an astronomical publication, Shkuratov (1988) suggested that coherent backscattering may play a role in producing the opposition brightening exhibited by a wide class of atmosphereless solar system bodies. Recently, Muinonen (1989, 1990) mentioned the opposition effect observed for Saturn's rings and the asteroid 44 Nysa as especially unusual and, probably, produced by the coherent backscattering mechanism, while Hapke (1990), Hapke and Blewett (1991) and Domingue *et al.* (1991) pointed out the coherent backscattering mechanism as possibly relevant to the strong and narrow opposition effect observed for icy outer planet satellites. Finally, Hapke *et al.* (1992) have found experimental evidence that coherent backscattering can contribute to the opposition effect of even such a low-albedo object as the Moon. However, no attempt has been made by these authors to apply relevant physical theories to quantitatively analyze the observed opposition phenomenon.

Coherent backscattering has been observed in laboratories for two kinds of scattering media, specifically for rough surfaces (e.g. McGurn, 1990; Maradudin *et al.*, 1992) and media composed of randomly positioned discrete scattering particles, e.g. powder-like layers or suspensions of latex particles in water (Kuga and Ishimaru, 1984; van Albada and Lagendijk, 1985; Wolf and Maret, 1985; Etemad *et al.*, 1986; Kaveh *et al.*, 1986). Unfortunately, theoretical and experimental results relevant to enhanced backscattering from random dielectric surfaces are extremely scarce. [Note that a freshly smoked magnesium oxide (MgO) sample studied by Kim *et al.*, 1990, was in fact a powder-like, three-dimensional discrete random medium rather than a real rough surface. Correspondingly, the measurements for this sample differ dramatically from the measurements by Sant *et al.*, 1989,

* Present address: NASA Goddard Institute for Space Studies, 2880 Broadway, New York, NY 10025, U.S.A.
Correspondence to: M. I. Mishchenko

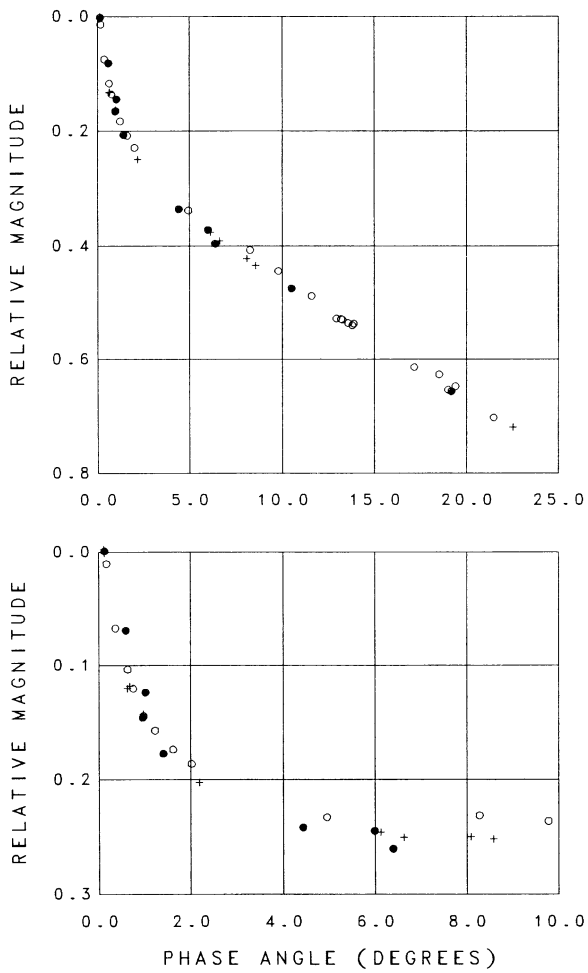

Fig. 1. The opposition effect for the asteroids 44 Nysa and 64 Angelina in the yellow (Harris *et al.*, 1989). The opposition spike on the lower panel is obtained after removal of a linear component of the phase curve

for a carefully fabricated rough dielectric surface.] Metal rough surfaces are studied in much more detail. However, unlike what was observed for E-type asteroids (Fig. 1), the angular width of the coherent backscattering peaks measured for metal surfaces (e.g. O'Donnell and Mendez, 1987; Kim *et al.*, 1990) was of about several degrees rather than several tenths of a degree, and the peaks were significantly rounded off near zero phase angle. Moreover, Sant *et al.* (1989) have demonstrated that scattering properties of metal and dielectric surfaces with identical roughness characteristics are quite different. Therefore, it is still not clear enough whether enhanced backscattering of light by dielectric rough surfaces can produce an opposition intensity peak similar to that observed for E-type asteroids (e.g. calculations by Antsygina *et al.*, 1991, demonstrate much broader and significantly rounded off peaks). On the other hand, it is well known that coherent backscattering of light from discrete random media can give rise to an opposition peak that has a distinct triangular shape near the opposition and half-width of only a few tenths of a degree. Thus, it is worthwhile to apply the theory of the latter phenomenon to interpret the astronomical observations.

The theory of coherent backscattering from discrete random media contains only reproducible physical parameters, has a rigorous theoretical background, and is in good quantitative agreement with the results of controlled laboratory experiments (see, e.g. Akkermans *et al.*, 1988; Wolf *et al.*, 1988; van der Mark *et al.*, 1988; Mishchenko, 1991c). In recent papers (Mishchenko and Dlugach, 1992b; Mishchenko, 1992b), we have shown that coherent backscattering of sunlight from a regolithic layer composed of submicrometer-sized ice grains is a likely explanation of the opposition effect exhibited by Saturn's A- and B-rings and icy outer planet satellites. It is the aim of the present paper to demonstrate that coherent backscattering can also explain the unusually narrow opposition effect observed for the asteroids 44 Nysa and 64 Angelina. For the reader's convenience, Section 2 will provide a brief introduction to the theory of coherent backscattering of light from discrete random media. For a much more thorough review of the subject, we refer the reader to Barabanenkov *et al.* (1991). Model calculations will be reported in Section 3. Finally, in Section 4 the principal results of the paper will be summarized and discussed.

2. Theory

To demonstrate the interference nature of coherent backscattering, let us first consider a half-space of randomly positioned scattering particles illuminated by a scalar plane wave incident in the direction given by the unit vector $\hat{\mathbf{n}}_i$ (Fig. 2). Let the direction of the reflected wave be given by the unit vector $\hat{\mathbf{n}}_r$. Consider two light-scattering paths shown in Fig. 2 by *solid and dashed lines*. These paths involve the same group of N scatterers, denoted by their positions $\mathbf{x}_1, \ldots, \mathbf{x}_N$, but the order of the scatterers is reversed. The waves scattered through the two paths will interfere, the interference being constructive or destructive depending on the phase difference between the paths $k(\hat{\mathbf{n}}_i + \hat{\mathbf{n}}_r)(\mathbf{x}_N - \mathbf{x}_1)$, where $k = 2\pi/\lambda$ is the wavenumber, and λ is the wavelength. Relatively far from the retroreflection direction, the waves scattered by different groups of particles through the conjugate couples of light paths will interfere in different ways, and, due to the randomness of the medium, the average effect of interference

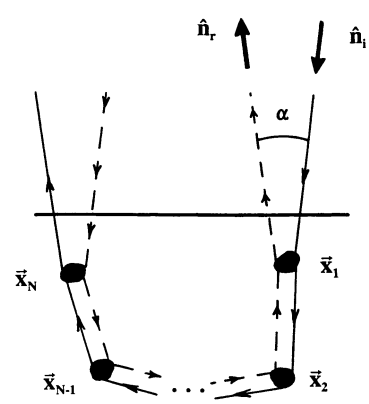

Fig. 2. Schematic explanation of coherent backscattering

will be zero. Nevertheless, at exactly the backscattering direction ($\hat{\mathbf{n}}_r = -\hat{\mathbf{n}}_i$), the phase difference between the conjugate light paths is identically equal to zero for any group of particles, and coherence is completely preserved. Owing to reciprocity, at exactly the backscattering direction, the amplitudes of the two light paths shown in Fig. 2 are equal ($A_1 = A_2$), and the reflected intensity is $|A_1+A_2|^2 = 4|A_1|^2$. In the absence of coherence, we would have for the backscattered intensity $|A_1|^2+|A_2|^2 = 2|A_1|^2$. Since the scattering paths that involve only one particle do not contribute to the coherent return (there is no reversed path), we conclude that, in the scalar approximation, coherence results in a backscattering peak of amplitude somewhat less than twice the incoherent intensity. More specifically, the backscattering enhancement factor ζ defined as the ratio of the total backscattered intensity to the incoherent (diffuse) intensity is given for exactly the backscattering direction by:

$$\zeta = \frac{I^{\mathrm{D}}+I^{\mathrm{C}}}{I^{\mathrm{D}}} = 2-\frac{I^{1}}{I^{\mathrm{D}}}, \tag{1}$$

where I^{D} is the diffuse intensity, I^{C} is the coherent contribution, and I^{1} is the contribution of the single-scattering paths.

Each of the two light scattering paths shown in Fig. 2 goes through each of the particles $\mathbf{x}_1, \ldots, \mathbf{x}_N$ only once. In the theory of multiple scattering of waves in discrete random media, such self-avoiding paths give rise to the so-called ladder and cyclical diagrams (see, e.g. Tsang *et al.*, 1985). The sum of the ladder diagrams describes the diffuse intensity I^{D}, while the sum of the cyclical diagrams describes the coherent contribution I^{C}. Unlike the diffuse intensity which is a slowly varying function of the phase angle α (the angle between the vectors $\hat{\mathbf{n}}_r$ and $-\hat{\mathbf{n}}_i$), the coherent contribution is nonzero only in the nearest vicinity of the pure backscattering direction. The contribution of all the other scattering paths, which go through the same scatterers more than once, is very small as compared with the contribution of the self-avoiding paths like those shown in Fig. 2 and may be neglected (e.g. Ishimaru, 1978). Furthermore, under particular conditions which will be discussed later, the incoherent intensity can be found by solving the common radiative transfer equation (Chandrasekhar, 1960; Ishimaru and Tsang, 1988). Calculation of the coherent contribution is a more difficult problem studied, e.g. by van der Mark *et al.* (1988), Gorodnichev *et al.* (1989, 1990), and Ozrin (1992a). However, as discussed above, at exactly the backscattering direction the coherent contribution is simply equal to the incoherent intensity minus the singly scattered intensity.

Although the scalar approximation gives reasonably good results in calculating the copolarized reflected intensity for linearly polarized incident light and in calculating the reflected intensity in the helicity-preserving channel for circularly polarized incident light (e.g. Etemad *et al.*, 1987; Wolf *et al.*, 1988), it does not take into account the vector character of light and, thus, provides only a simplified understanding of coherent backscattering. In particular, the scalar approximation completely fails in calculating the reflected intensity in the practically important case of unpolarized incident light (Mishchenko and Dlugach, 1992a).

In accordance with the vector nature of light, the scalar intensity must be replaced by the four-component Stokes vector $[\mathbf{I}]$ having the Stokes parameters as its components, as follows:

$$[\mathbf{I}] = \begin{bmatrix} I \\ Q \\ U \\ V \end{bmatrix}. \tag{2}$$

The Stokes vector of the reflected light $[\mathbf{I}^{\mathrm{r}}]$ is given by:

$$[\mathbf{I}^{\mathrm{r}}] = [\mathbf{R}][\mathbf{I}^{\mathrm{i}}], \tag{3}$$

where $[\mathbf{R}]$ is the (4×4) reflection matrix, and $[\mathbf{I}^{\mathrm{i}}]$ is the Stokes vector of the incident light. As in the scalar case, the diffuse component of the reflection matrix $[\mathbf{R}^{\mathrm{D}}]$ can be calculated by using the vector radiative transfer theory (e.g. Hansen and Travis, 1974; Hovenier and van der Mee, 1983; Tsang *et al.*, 1985). On the other hand, calculation of the coherent component $[\mathbf{R}^{\mathrm{C}}]$ is a more difficult problem which is rigorously solved only for particles much smaller than the wavelength, i.e. Rayleigh scatterers (Ozrin, 1992b). However, as was shown by Mishchenko (1992a), at exactly the backscattering direction the coherent component $[\mathbf{R}^{\mathrm{C}}]$ can be rigorously expressed in terms of the matrix $[\mathbf{R}^{\mathrm{L}}] = [\mathbf{R}^{\mathrm{D}}]-[\mathbf{R}^{1}]$, where, as earlier, $[\mathbf{R}^{1}]$ is the contribution of the singly scattered light. The matrix $[\mathbf{R}^{\mathrm{L}}]$ describes the diffuse contribution of all the self-avoiding paths that include more than one scatterer, i.e. the contribution of all the ladder diagrams of orders $N \geqslant 2$. For macroscopically isotropic scattering media, this expression has the form:

$$[\mathbf{R}^{\mathrm{C}}] = \begin{bmatrix} R^{\mathrm{C}}_{11} & R^{\mathrm{L}}_{12} & 0 & 0 \\ R^{\mathrm{L}}_{12} & R^{\mathrm{C}}_{22} & 0 & 0 \\ 0 & 0 & R^{\mathrm{C}}_{33} & R^{\mathrm{L}}_{34} \\ 0 & 0 & -R^{\mathrm{L}}_{34} & R^{\mathrm{C}}_{44} \end{bmatrix}, \tag{4}$$

with:

$$R^{\mathrm{C}}_{11} = \tfrac{1}{2}[R^{\mathrm{L}}_{11}+R^{\mathrm{L}}_{22}-R^{\mathrm{L}}_{33}+R^{\mathrm{L}}_{44}], \tag{5}$$

$$R^{\mathrm{C}}_{22} = \tfrac{1}{2}[R^{\mathrm{L}}_{11}+R^{\mathrm{L}}_{22}+R^{\mathrm{L}}_{33}-R^{\mathrm{L}}_{44}], \tag{6}$$

$$R^{\mathrm{C}}_{33} = \tfrac{1}{2}[-R^{\mathrm{L}}_{11}+R^{\mathrm{L}}_{22}+R^{\mathrm{L}}_{33}+R^{\mathrm{L}}_{44}], \tag{7}$$

$$R^{\mathrm{C}}_{44} = \tfrac{1}{2}[R^{\mathrm{L}}_{11}-R^{\mathrm{L}}_{22}+R^{\mathrm{L}}_{33}+R^{\mathrm{L}}_{44}]. \tag{8}$$

Thus, for the case of unpolarized incident light, the scalar formula (1) for the backscattering enhancement factor ζ at exactly the backscattering direction is replaced by the vector formula:

$$\zeta = \frac{[R^{1}_{11}+R^{\mathrm{L}}_{11}+R^{\mathrm{C}}_{11}]}{[R^{1}_{11}+R^{\mathrm{L}}_{11}]} = \frac{[R^{1}_{11}+R^{\mathrm{L}}_{11}+\tfrac{1}{2}(R^{L}_{11}+R^{\mathrm{L}}_{22}-R^{\mathrm{L}}_{33}+R^{\mathrm{L}}_{44})]}{[R^{1}_{11}+R^{\mathrm{L}}_{11}]}. \tag{9}$$

The expression (4) is a direct consequence of the vector theory of multiple wave scattering in discrete random media and is based on Saxon's (1955) reciprocity relation for the single-scattering amplitude matrix. As was demonstrated by Mishchenko (1991c), this theory is in good quantitative agreement with the controlled laboratory

measurements made by Wolf *et al.* (1988) and van Albada *et al.* (1988) for densely packed latex particles in water illuminated by linearly polarized incident light. Also, for the case of circularly polarized incident light and the helicity-preserving channel, this theory predicts the enhancement factor of exactly two regardless of the effects of finite geometry and absorption, which is in full agreement with measurements of Etemad *et al.* (1987). Finally, calculations by Mishchenko (1991c, 1992a) for point-like particles show complete agreement with the numbers given by Ozrin (1992b) on the basis of his rigorous vector theory of coherent backscattering by Rayleigh scatterers.

Thus, the calculation of the amplitude of the coherent opposition effect consists of two steps. First, the diffuse reflection matrix $[\mathbf{R}^{\mathrm{D}}]$ and the single-scattering contribution $[\mathbf{R}^{1}]$ are calculated by using the well-known numerical methods of the radiative transfer theory. At present, numerical calculations are possible for spherical (Hansen, 1971; Hansen and Travis, 1974; de Haan *et al.*, 1987) as well as for randomly oriented nonspherical (Mishchenko, 1991a,b; Wauben and Hovenier, 1992) particles. Subsequently, equation (9) is used.

It must be noted that the use of the radiative transfer theory to calculate the diffuse component of the reflection matrix and the use of equation (9) to calculate the backscattering enhancement factor imply that the scattering medium consists of uncorrelated, independently scattering particles. In this case, the longitudinal component of the electric field becomes negligibly small. However, as was demonstrated by Mishchenko (1991c) by comparing theoretical calculations with results of controlled laboratory experiments, the approximation of independent scattering gives good quantitative results even for rather densely packed media. Furthermore, as was shown by Tsang *et al.* (1990), for densely packed media the incoherent component of the Stokes vector of multiply scattered light is a solution of an equation which has the same form as the classical radiative transfer equation and contains the same phase matrix, but the extinction coefficient and single-scattering albedo are modified. However, for the diffuse reflection matrix of a semi-infinite nonabsorbing medium, this modified radiative transfer equation gives exactly the same results as the classical radiative transfer equation. Since calculations reported in the next section are made for optically thick (semi-infinite) media composed of nonabsorbing particles, we expect that the accuracy of our computations is good enough for the purposes of interpretation.

We stress here that the theory developed by Mishchenko (1992a) is based, in the last analysis, on Maxwell's equations. Although it includes a simplifying assumption of independent scattering, this assumption is explicit and is not accompanied by the introduction of adjustable model parameters without definite physical meaning. The same is true for the radiative transfer theory, which is a direct consequence of the Bethe–Salpeter equation under the ladder approximation for independent scatterers (Barabanenkov, 1975; Prishivalko *et al.*, 1984; Tsang *et al.*, 1985).

Thus, the radiative transfer theory and equation (9) enable us to rather accurately calculate the intensity of the reflected light both in the centre of the coherent opposition peak and outside the peak. To have more complete specification of the peak, we must also calculate its half-width at half-maximum (HWHM). As was rigorously shown by Ozrin (1992b) for the case of a semi-infinite medium composed of nonabsorbing Rayleigh (point-like) scatterers and illuminated by a parallel beam of light incident perpendicularly to the boundary of the medium, the coherent component of the reflected light in the vicinity of exactly the backscattering direction depends on the phase angle α only through the angular parameter $q = kl\alpha$, where l is the scattering mean free path of photons in the medium. Figure 3 shows the angular profile of the backscattering enhancement factor ζ_{R} calculated on the basis of the Ozrin theory for the case of unpolarized incident light (Mishchenko, 1993). Note that $\zeta_{\mathrm{R}}(0) \approx 1.54$ (*cf.* Mishchenko, 1992a). It is seen from this figure that the HWHM of the coherent opposition peak is given by:

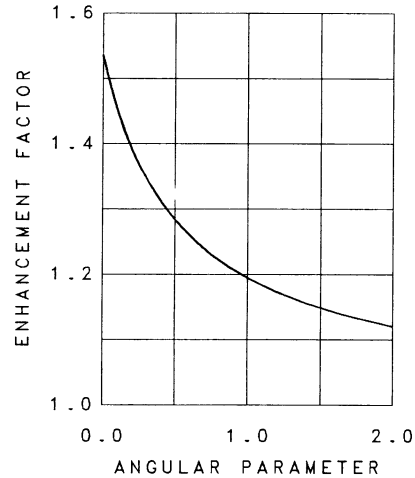

Fig. 3. Enhancement factor ζ vs angular parameter q for a semi-infinite random medium composed of nonabsorbing point-like scatterers and illuminated by unpolarized, perpendicularly incident light

$$\mathrm{HWHM} \approx \frac{0.56}{kl} = \frac{0.56\lambda}{2\pi l}. \tag{10}$$

The proportionality of HWHM to the ratio λ/l is a direct consequence of the interference nature of coherent backscattering and has been verified in a lot of controlled laboratory experiments (e.g. Wolf *et al.*, 1988). As follows from the theory of coherent backscattering (e.g. Akkermans *et al.*, 1988; Ozrin, 1992a), in the case of finite-sized, anisotropically scattering grains, the scattering mean free path l must be replaced by the transport mean free path l_{tr} given by $l/(1-g)$, where g is the asymmetry parameter of the phase function (for Rayleigh scatterers, $g = 0$ and $l_{\mathrm{tr}} = l$). Calculation of the transport mean free path and HWHM for sparsely packed media is rather straightforward. However, calculations for realistic, densely packed media require special attention since spatial correlation among scatterers can lead to a substantial increase of l_{tr} as compared with sparsely distributed particles. Calculations of l_{tr} and HWHM on the basis of a dense-medium light-scattering theory, in which spatial correlation among scatterers is taken into account by intro-

ducing the so-called static structure factor (Balescu, 1975), are described, e.g. by Wolf *et al.* (1988) and Mishchenko (1992b). As is shown by Wolf *et al.* (1988) this theory gives good quantitative agreement with the results of their laboratory experiments.

It should be emphasized that coherent backscattering is an essentially cooperative, multiple-scattering phenomenon resulting from the electromagnetic interaction of all the particles forming the scattering medium. This is especially true for nonabsorbing or weakly absorbing media because in this case most of the reflected photons undergo a lot of scattering events and, thus, their path within the medium is much longer than the mean distance between the scattering particles. Therefore, it is hardly expected that simple, geometrically confined scattering configurations containing only a few particles (e.g. Muinonen, 1989; Muinonen and Lumme, 1991; Tishkovets and Shkuratov, 1992) or a single Rayleigh particle above an interface (Muinonen *et al.*, 1991) can provide relevant quantitative description of the coherent backscatter opposition effect exhibited by high-albedo atmosphereless surfaces (Saturn's rings, icy outer planet satellites, E-type asteroids), although they enable one to accurately take into account the longitudinal component of the electric field, and some of them may be useful in explaining the negative polarization branch observed for cometary dust. As was shown by Etemad *et al.* (1987) and Wolf *et al.* (1988), the main effect of confined geometry on light scattering is to round off the coherent peak which, for optically thick nonabsorbing media, has a distinct triangular shape near the opposition (Fig. 3). And indeed, all the coherent backscattering peaks calculated by Muinonen *et al.* (1991) are (strongly) rounded off (it should be noted, however, that Muinonen *et al.* pointed out themselves that their emphasis was not on detailed but rather on broad-minded modeling of natural circumstances).

Finally, we note that, recently, a vector theory of coherent backscattering has been proposed by Peters (1992) for absorbing and nonabsorbing particles of size comparable to a wavelength. Comparison with Mishchenko (1992c) shows that Peters' calculations for Rayleigh (point-like) scatterers are reasonably accurate. However, several rather crude approximations are made in this theory, and, as a result, particle size and refractive index are not explicit model parameters and may affect the intensity and polarization of multiply scattered light only through the scattering and absorption cross-sections and mean cosine of the scattering angle, which does not seem physically realistic. Also, this makes it difficult to verify Peters' theory vs the results of controlled laboratory experiments or alternative theoretical calculations.

3. Calculations

As was pointed out above, we assume that the surface of the asteroids 44 Nysa and 64 Angelina is (partly) covered with a layer of small regolithic grains producing the observed opposition effect via the coherent backscattering mechanism. For simplicity, we assume that the regolithic grains are homogeneous spheres with radii governed by the standard gamma distribution (Hansen and Hovenier, 1974):

$$n(r) \propto r^{(1-3b)/b} \exp[-r/(ab)], \tag{11}$$

where a is the effective radius and b is the effective variance. Also, we assume that the regolithic layer is optically thick (semi-infinite), the regolithic particles are nonabsorbing or weakly absorbing, and their index of refraction is in the interval [1.6, 1.7]. These assumptions are motivated by the following two reasons.

(1) Both 44 Nysa and 64 Angelina are high-albedo asteroids, and their surface is generally believed to be composed of a transparent dielectric material similar to the mineral enstatite with an index of refraction near 1.66 (e.g. Zellner, 1975; Zellner *et al.*, 1977; Clotius *et al.*, 1990).

(2) Both absorption and the finite optical thickness of the scattering layer result in (strong) rounding off of the coherent backscattering peak (e.g. Etemad *et al.*, 1987; Wolf *et al.*, 1988), which otherwise has a distinct triangular shape near exactly the backscattering direction (Fig. 3). The measurements of Harris *et al.* (1989), which are characterized by a very small scatter of data points, do not show such a rounding off (Fig. 1). Therefore, it is reasonable to assume that at least those parts of the surface of the asteroids that are responsible for the observed opposition brightening are covered with an optically thick layer composed of nonabsorbing (or weakly absorbing) grains.

As is seen from Figs 1 and 3, the observed opposition peak has the same shape as that calculated from the theory of coherent backscattering. Therefore, to show that coherent backscattering of sunlight by the small regolithic grains can explain the unusually narrow opposition effect observed for the asteroids in the yellow, we must reproduce theoretically the observed amplitude of about 0.25 mag and angular semi-width of about 0.8° (see Fig. 1, lower panel).

The angular semi-width of the coherent opposition peak depends on four model parameters: the (real) refractive index N of the regolithic grains, a dimensionless size parameter y defined as the ratio of the effective grain radius to the wavelength of light, the effective variance b, and filling factor f (i.e. the fraction of a volume occupied by the grains). In Figs 4–6, HWHM is plotted vs y for different values of f, b and N. In our calculations, we used a dense-medium light-scattering theory based on introducing the static structure factor (e.g. Wolf *et al.*, 1988; Mishchenko, 1992b). It is seen from Figs 4–6, that whatever the grain refractive index is, HWHM has a peak near $y = 0.5$. The amplitude of the peak increases with increasing filling factor, decreasing width of the particle size distribution specified by the effective variance b, and increasing refractive index. HWHM tends to zero with either $y \to 0$ or $y \to \infty$. In practice this means that the coherent backscattering peak becomes unobservable for regolithic grains either much smaller or much larger than the wavelength. For $y > 1$, HWHM is almost independent of N.

Unfortunately, Harris *et al.* (1989) report only yellow

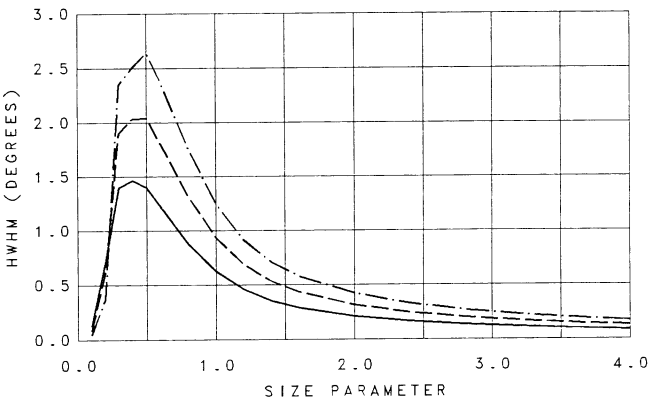

Fig. 4. Angular semi-width of the coherent backscatter opposition effect vs a dimensionless size parameter $y = a/\lambda$ for the refractive index $N = 1.65$, effective variance $b = 0.1$ and filling factors $f = 0.2$ (*solid curve*), 0.3 (*dashed curve*) and 0.4 (*dot–dashed curve*)

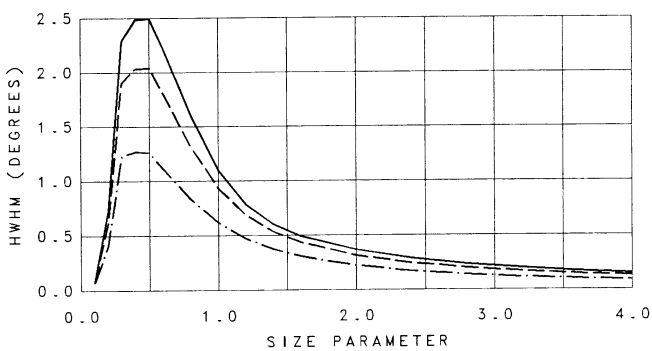

Fig. 5. The same as in Fig. 4 for $N = 1.65$, $f = 0.3$ and $b = 0.05$ (*solid curve*), 0.1 (*dashed curve*) and 0.2 (*dot–dashed curve*)

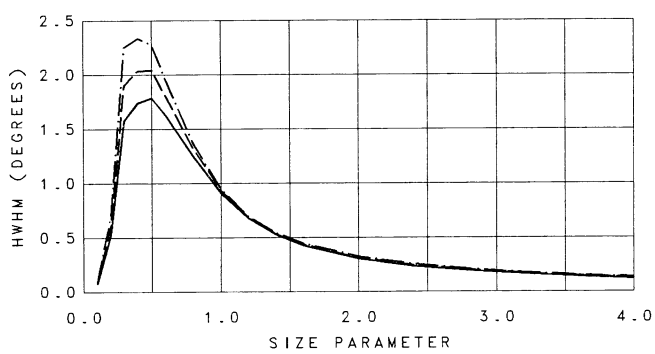

Fig. 6. The same as in Fig. 4 for $b = 0.1$, $f = 0.3$ and $N = 1.6$ (*solid curve*), 1.65 (*dashed curve*) and 1.7 (*dot–dashed curve*)

(V) magnitudes of the opposition effect for 44 Nysa and 64 Angelina. This makes the inversion problem ill posed and does not enable us to determine uniquely the size and refractive index of the grains producing the opposition effect. However, it is seen from Figs 4–6 that dielectric grains with index of refraction close to that of the mineral enstatite and effective radii from roughly 0.2 μm to roughly 0.7 μm can explain the observed angular semi-width of about 0.8°.

It should be noted here that the curves in Figs 4–6 are calculated for the case of normal incidence of light on the surface. In the case of oblique incidence (e.g. near the limbs or due to macroscopic surface roughness), HWHM increases as $1/\cos\vartheta$ (Gorodnichev *et al.*, 1990), where ϑ is the angle of incidence measured from the inward normal to the surface. Therefore, for a three-dimensional body with a macroscopically rough surface, the observed angular semi-width will be somewhat larger than that given by equation (10). Although it is practically impossible to calculate this enlargement accurately, a factor of about 1.5 seems to be a reasonable upper limit. Indeed, for a smooth, spherically symmetric body, the angle of incidence averaged over the illuminated surface at zero phase is equal to 45°, thus implying a factor of 1.4. The same factor follows from the assumption that rms surface roughness is close to 45° (e.g. Lumme *et al.*, 1985). Obviously, the combined effect of the global asteroid shape and surface roughness at zero phase will result in approximately the same or even weaker enlargement. As is seen from Figs 4–6, such an enlargement practically does not change the lower limit of possible grain radii, but slightly raises the upper limit.

The second quantity that specifies the opposition effect is the amplitude of the opposition spike $\tilde{\zeta}$, which is defined as the ratio of the total (i.e. diffuse+coherent) backscattered intensity at zero phase angle to the diffuse, background intensity:

$$\tilde{\zeta} = I_{\text{total}}/I_{\text{diffuse}} = [I_{\text{diffuse}} + I_{\text{coherent}}]/[I_{\text{diffuse}}]. \qquad (12)$$

In the case of a macroscopically flat surface uniformly covered with the grains producing the coherent opposition effect, $\tilde{\zeta} = \zeta$, where ζ is given by equation (9). However, in the case of a (supposedly) nonuniform and macroscopically rough surface of the asteroids, $\tilde{\zeta}$ will be smaller than ζ. Indeed, in this case the backscattered light can be divided into two parts of different origin. The first part comes from the light that is singly reflected in the opposite direction by unshadowed surface elements composed of the submicrometer-sized grains. This backscattered light results from the multiple-scattering processes that occur inside individual unshadowed surface elements with size of the order of the transport mean free path l_{tr}. These multiple-scattering processes both contribute to the diffuse intensity and give rise to the observed coherent backscattering peak with HWHM $\simeq 0.8°$. The second part is the light that is (i) scattered by the surface elements composed of grains either much smaller or much larger than the wavelength and (ii) the light that is multiply reflected by different surface elements. These multiple reflections arise due to macroscopic surface roughness with scale much greater than l_{tr}. The second part of the backscattered light contributes to the diffuse intensity but does not contribute to the observed opposition peak.

Precise calculations of the two components of the backscattered intensity are difficult because they require detailed information about the large-scale surface roughness, the fraction of the surface covered with the submicrometer-sized grains, and the size of the grains that cover the rest of the surface. Therefore, the only thing that we can do now is to verify that the observed amplitude of the opposition effect $\tilde{\zeta}$ is smaller than the amplitude ζ calculated theoretically for the light singly reflected by a

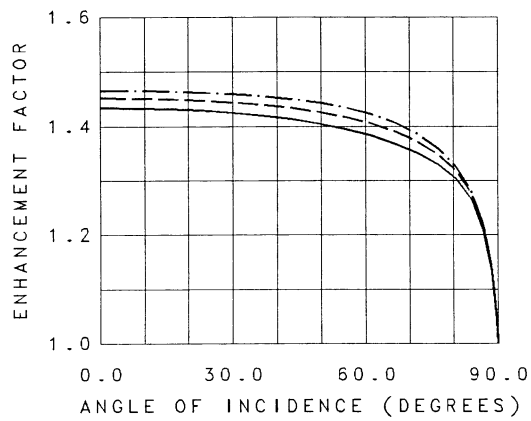

Fig. 7. The theoretically computed amplitude of the opposition effect ζ vs the angle of incidence. The optically thick (semi-infinite) medium with macroscopically flat surface is composed of polydisperse spherical particles with $a/\lambda = 1$, $N = 1.65$ and $b = 0.05$ (*solid curve*), 0.1 (*dashed curve*) and 0.2 (*dot–dashed curve*)

macroscopically flat surface uniformly covered with the submicrometer-sized grains.

Theoretical calculations based on equation (9) have shown that, in the range $0.25 \leqslant y \leqslant 3$, the amplitude ζ is practically independent of the effective variance b. In Fig. 7, ζ is plotted vs the angle of incidence ϑ (measured from the inward normal to the surface) for $y = 1$, $N = 1.65$ and $b = 0.05$, 0.1 and 0.2. It is seen that up to $\vartheta \simeq 80°$, ζ is a very slowly decreasing function of ϑ. In Fig. 8, the enhancement factor for normal incidence $\zeta(0)$ is plotted vs the size parameter y for $b = 0.1$ and $N = 1.6$, 1.65 and 1.7. Indeed we see that, in accordance with the conclusion of the preceding paragraph, the theoretically calculated amplitudes of about 1.4–1.6 are larger than the observed amplitude of about 0.25 mag in the yellow (Harris *et al.*, 1989). This means that the fraction of the surface covered by the submicrometer-sized grains producing the opposition effect is less than unity and/or the multiple-reflection

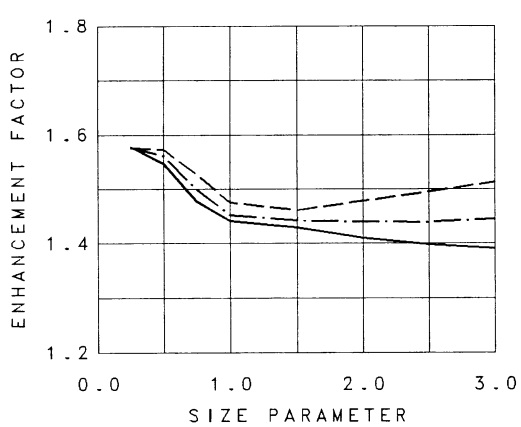

Fig. 8. The amplitude of the opposition effect for normal incidence $\zeta(0)$ vs the size parameter y for $b = 0.1$ and $N = 1.6$ (*dashed curve*), 1.65 (*dot–dashed curve*) and 1.7 (*solid curve*)

contribution due to macroscopic surface roughness is comparable with the single-reflection contribution.

4. Discussion and conclusions

Thus, we have shown in this paper that coherent backscattering of sunlight from an upper regolithic layer which, apparently, partly covers the surfaces of the asteroids 44 Nysa and 64 Angelina and is composed of submicrometer-sized silicate grains, can produce the observed narrow and strong opposition spikes. We did not try here to find a unique solution for the parameters that specify the submicrometer-sized regolithic grains: a, b, N, f, and the fraction of the surface covered with these grains. Unfortunately, the observational data are not sufficient for this purpose. These parameters influence both the angular width and amplitude of the opposition spike, and the effect of one of these parameters can be compensated for by the effect of others. However, in our calculations we used a physical theory that has a rather strong physical background, involves direct physical parametrization in terms of the reproducible parameters a, b, N and f, and has been verified in a lot of controlled laboratory experiments. Thus, although we were not able to prove that coherent backscattering *is* the explanation of the remarkable opposition brightening, we have demonstrated quantitatively that coherent backscattering *can* be a realistic explanation of this phenomenon.

As follows from our calculations, to produce the observed opposition peak via the coherent backscattering mechanism, the grains should have sizes of the order of the wavelength. Much larger or much smaller grains produce a coherent peak that is too narrow to be observed. It was shown in our recent paper (Mishchenko and Dlugach, 1992b) that the opposition effect observed for Saturn's rings in the visible is, apparently, due to coherent backscattering of sunlight from a layer of submicrometer-sized ice grains which (partially) covers macroscopic ring particles. The same grains are known to produce the famous radial spokes in the outer B-ring of Saturn (Doyle and Grün, 1990) and may be responsible for the remarkable opposition effect observed for Europa and icy Uranian satellites (Mishchenko, 1992b). The possible origin of the submicrometer-sized regolithic grains at ice-covered atmosphereless surfaces at low temperatures is discussed by Smoluchowski (1983). It is still not clear if regolithic grains of the same size may be present at silicate airless surfaces. It is usually suggested that regolithic particles produced by meteoritic bombardment have radii of about 10 μm at the surface of the Moon and Mercury, and are much coarser at the surface of asteroids (e.g. Dollfus *et al.*, 1989). However, as was shown by Zook and McCoy (1991), parts of the lunar surface may be covered by much finer, submicrometer-sized dust grains. If these grains are produced by a physical mechanism different from that discussed by Dollfus *et al.*, it may well be that the same submicrometer-sized grains are also present on the surface of the asteroids 44 Nysa and 64 Angelina.

Finally we note that, as follows from Figs 4–6, the angular semi-width of the coherent backscatter opposition

effect is wavelength dependent. Therefore, spectral measurements of the opposition effect for the asteroids 44 Nysa and 64 Angelina would test if coherent backscattering is a likely explanation of the observed opposition spike and provide additional constraints on the size of the regolithic grains.

Acknowledgements. We are indebted to E. G. Yanovitskij, L. O. Kolokolova, L. R. Lisina, R. Smoluchowski, Yu. G. Shkuratov and B. Cairns for useful discussions, and to J. E. Geake and an anonymous reviewer for valuable comments on preliminary versions of this paper. We thank A. Walker and A. Wolf for programming support and Z. Wai for technical assistance. MIM gratefully acknowledges support from P. C. Day, H. T. Johnson, M. Sotman and J. H. Tietjen.

References

Akkermans, E., Wolf, P. E., Maynard, R. and Maret, G., Theoretical study of the coherent backscattering of light by disordered media, *J. Phys.* (*Paris*) **49,** 77–98, 1988.

Antsygina, T. N., Freylikher, V. D., Gredeskul, S. A., Pastur, L. A. and Slusarev, V. A., Backscattering enhancement by an impedance surface, *J. Electro. Waves Applic.* **8,** 873–884, 1991.

Balescu, R., *Equilibrium and Nonequilibrium Statistical Mechanics*, Wiley, New York, 1975.

Barabanenkov, Yu. N., Multiple scattering of waves by ensembles of particles and the theory of radiation transport, *Sov. Phys.-Usp.* **18,** 673–689, 1975.

Barabanenkov, Yu. N., Kravtsov, Yu. A., Ozrin, V. D. and Saichev, A. I., Enhanced backscattering in optics, in *Progress in Optics XXIX* (edited by E. Wolf), pp. 67–197, Elsevier, Amsterdam, 1991.

Brown, R. H. and Cruikshank, D. P., The Uranian satellites and Hyperion: new spectrophotometry and compositional implications, *Icarus* **56,** 414–425, 1983.

Buratti, B. J., Ganymede and Callisto: surface textural dichotomies and photometric analysis, *Icarus* **92,** 312–323, 1991.

Chandrasekhar, S., *Radiative Transfer*, Dover, New York, 1960.

Clotius, E. A., Gaffey, M. J., Smith, D. G. V. and Lambert, R. S. T., Reflectance spectra of "featureless" materials and the surface mineralogies of M- and E-class asteroids, *J. geophys. Res.* **95,** 281–293, 1990.

de Haan, J. F., Bosma, P. B. and Hovenier, J. W., The adding method for multiple scattering calculations of polarized light, *Astron. Astrophys.* **183,** 371–391, 1987.

Dollfus, A., Wolff, M., Geake, J. E., Lupishko, D. F. and Dougherty, L. M., Photopolarimetry of asteroids, in *Asteroids II* (edited by R. P. Binzel, T. Gehrels and M. S. Matthews), pp. 594–616, University of Arizona Press, Tucson, AZ, 1989.

Domingue, D. L., Hapke, B. W., Lockwood, G. W. and Thompson, D. T., Europa's phase curve: implications for surface structure, *Icarus* **90,** 30–42, 1991.

Doyle, L. R. and Grün, E., Radiative transfer modeling constraints on the size of the spoke particles in Saturn's rings, *Icarus* **85,** 168–190, 1990.

Etemad, S., Thompson, R and Andrejco, M. J., Weak localization of photons: universal fluctuations and ensemble averaging, *Phys. Rev. Lett.* **57,** 575–578, 1986.

Etemad, S., Thompson, R., Andrejco, M. J., John, S. and MacKintosh, F. C., Weak localization of photons: termination of coherent random walks by absorption and confined geometry, *Phys. Rev. Lett.* **59,** 1420–1423, 1987.

Franklin, F. A. and Cook, A. F., Optical properties of Saturn's rings. II. Two-color phase curves of the two bright rings, *Astron. J.* **70,** 704–720, 1965.

Goguen, J. D., Hammel, H. B. and Brown, R. H., V photometry of Titania, Oberon, and Triton, *Icarus* **77,** 239–247, 1989.

Gorodnichev, E. E., Dudarev, S. L. and Rogozkin, D. B., Coherent backscattering enhancement under condition of weak localization in three-dimensional and two-dimensional disordered systems, *Zh. Eksper. Teor. Fiz.* **96,** 847–864, 1989.

Gorodnichev, E. E., Dudarev, S. L. and Rogozkin, D. B., Coherent wave backscattering by random medium. Exact solution of the albedo problem. *Phys. Lett.* **144,** 48–54, 1990.

Hansen, J. E., Multiple scattering of polarized light in planetary atmospheres. Part II. Sunlight reflected by terrestrial water clouds, *J. Atmos. Sci.* **28,** 1400–1426, 1971.

Hansen, J. E. and Hovenier, J. W., Interpretation of the polarization of Venus, *J. Atmos. Sci.* **31,** 1137–1159, 1974.

Hansen, J. E. and Travis, L. D., Light scattering in planetary atmospheres, *Space Sci. Rev.* **16,** 527–610, 1974.

Hapke, B., Bidirectional reflectance spectroscopy: 4. The extinction coefficient and the opposition effect, *Icarus* **67,** 264–280, 1986.

Hapke, B., Coherent backscatter and the radar characteristics of outer planet satellites, *Icarus* **88,** 407–417, 1990.

Hapke, B. and Blewett, D., Coherent backscatter model for the unusual radar reflectivity of icy satellites, *Nature* **352,** 46–47, 1991.

Hapke, B., Nelson, R. and Smythe, W., The opposition effect of the Moon: coherent backscatter, *Bull. Amer. Astron. Soc.* **24,** 1021, 1992.

Harris, A. W., Young, J. M., Contreiras, L., Dockweiler, T., Belkora, L., Salo, H., Harris, W. D., Bowell, E., Poutanen, M., Binzel, R. P., Tholen, D. J. and Wong, S., Phase relations of high albedo asteroids: the unusual opposition brightening of 44 Nysa and 64 Angelina, *Icarus* **81,** 365–374, 1989.

Hovenier, J. W. and van der Mee, C. V. M., Fundamental relationships relevant to the transfer of polarized light in a scattering atmosphere, *Astron. Astrophys.* **128,** 1–16, 1983.

Ishimaru, A., *Wave Propagation and Scattering in Random Media, Vol. 2. Multiple Scattering, Turbulence, Rough Surfaces and Remote Sensing*, Academic Press, New York, 1978.

Ishimaru, A. and Tsang, L., Backscattering enhancement of random discrete scatterers of moderate sizes, *J. Opt. Soc. Amer. A* **5,** 228–236, 1988.

Kaveh, M., Rosenbluh, M., Edrei, I. and Freund, I., Weak localization and light scattering from disordered solids, *Phys. Rev. Lett.* **57,** 2049–2052, 1986.

Kim, M.-J., Dainty, J. C., Friberg, A. T. and Sant, A. J., Experimental study of enhanced backscattering from one- and two-dimensional random rough surfaces, *J. Opt. Soc. Amer. A* **7,** 569–577, 1990.

Kuga, Y. and Ishimaru, A., Retroreflectance from a dense distribution of spherical particles, *J. Opt. Soc. Amer. A* **1,** 831–835, 1984.

Lagerkvist, C.-I., Magnusson, P., Williams, I. P., Buontempo, M. E., Argyle, R. W. and Morrison, L. V., Physical studies of asteroids. XXIV. Phase relations for 48 asteroids obtained with the Carlsberg Meridian Circle, *Astron. Astrophys. Suppl. Ser.* **94,** 43–71, 1992.

Lumme, K. and Bowell, E., Radiative transfer in the surfaces of atmosphereless bodies. I. Theory, *Astron. J.* **86,** 1694–1704, 1981.

Lumme, K., Karttunen, H. and Irvine, W. M., Roughness of the lunar soil, *Earth, Moon, Planets* **33,** 19–29, 1985.

Maradudin, A. A., Lu, J. Q., Tran, P., Wallis, R. F., Celli, V., Gu, Z.-H., McGurn, A. R., Méndez, E. R., Michel, T., Nieto-Vesperinas, M., Dainty, J. C. and Sant, A. J., Enhanced backscattering from one- and two-dimensional surfaces, *Rev. Mex. Fís.* **38,** 343–397, 1992.

McGurn, A. R., Enhanced retroreflectance effects in the reflection of light from randomly rough surfaces, *Surf. Sci. Rep.* **10,** 357–410, 1990.

Mishchenko, M. I., Light scattering by randomly oriented axially symmetric particles, *J. Opt. Soc. Amer. A* **8,** 871–882, 1991a.

Mishchenko, M. I., Reflection of polarized light by plane-parallel slabs containing randomly-oriented, nonspherical particles, *J. Quant. Spectrosc. Radiat. Transfer* **46,** 171–181, 1991b.

Mishchenko, M. I., Polarization effects in weak localization of light: calculation of the copolarized and depolarized enhancement factors, *Phys. Rev. B* **44,** Rapid communication, 12597–12600, 1991c.

Mishchenko, M. I., Enhanced backscattering of polarized light from discrete random media: calculations in exactly the backscattering direction, *J. Opt. Soc. Amer. A* **9,** 978–982, 1992a.

Mishchenko, M. I., The angular width of the coherent backscatter opposition effect: an application to icy outer planet satellites, *Astrophys. Space Sci.* **194,** 327–333, 1992b.

Mishchenko, M. I., Polarization characteristics of the coherent backscatter opposition effect, *Earth, Moon, Planets* **58,** 127–144, 1992c.

Mishchenko, M. I., On the nature of the polarization opposition effect exhibited by Saturn's rings, *Astrophys. J.*, 1993 (in press).

Mishchenko, M. I. and Dlugach, J. M., The amplitude of the opposition effect due to weak localization of photons in discrete random media, *Astrophys. Space Sci.* **189,** 151–154, 1992a.

Mishchenko, M. I. and Dlugach, J. M., Can weak localization of photons explain the opposition effect of Saturn's rings? *Mon. Not. Royal Astron. Soc.* **254,** 15p–18p, 1992b.

Muinonen, K., Electromagnetic scattering by two interacting dipoles, in *Proc.* 1989 *URSI EM Theory Symp.*, Stockholm, pp. 428–430, 1989.

Muinonen, K., Light scattering by inhomogeneous media: backward enhancement and reversal of linear polarization, Ph.D. thesis, University of Helsinki, 1990.

Muinonen, K. and Lumme, K., Light scattering by a randomly oriented cluster of spheres, *Bull. Amer. Astron. Soc.* **23,** 1144, 1991.

Muinonen, K. O., Sihvola, A. H., Lindell, I. V. and Lumme, K. A., Scattering by a small object close to an interface. II. Study of backscattering, *J. Opt. Soc. Amer. A* **8,** 447–482, 1991.

O'Donnell, K. A. and Mendez, E. R., Experimental study of scattering from characterized random surfaces, *J. Opt. Soc. Amer. A* **4,** 1194–1205, 1987.

Ozrin, V. D., Exact solution for coherent backscattering from a semi-infinite random medium of anisotropic scatterers, *Phys. Lett. A* **162,** 341–345, 1992a.

Ozrin, V. D., Exact solution for coherent backscattering of polarized light from a random medium of Rayleigh scatterers, *Waves Random Med.* **2,** 141–164, 1992b.

Peters, K. J., Coherent-backscatter effect: a vector formulation accounting for polarization and absorption effects and small or large scatterers, *Phys. Rev. B* **46,** 801–812, 1992.

Prishivalko, A. P., Babenko, V. A. and Kuz'min, V. N., *Scattering and Absorption of Light by Inhomogeneous and Anisotropic Spherical Particles*, Nauka i Tekhnika, Minsk, 1984.

Sant, A. J., Dainty, J. C. and Kim, M.-J., Comparison of surface scattering between identical, randomly rough metal and dielectric diffusers, *Opt. Lett.* **14,** 1183–1185, 1989.

Saxon, D. S., Tensor scattering matrix for the electromagnetic field, *Phys. Rev.* **100,** 1771–1775, 1955.

Shkuratov, Yu. G., Diffractional model of the brightness surge of complex structure surfaces, *Kin. Fiz. Nebes. Tel* **4,** 33–39, 1988.

Smoluchowski, R., Formation of fine dust on Saturn's rings as suggested by the presence of spokes, *Icarus* **54,** 263–266, 1983.

Thompson, D. T. and Lockwood, G. W., Photoelectric photometry of Europa and Callisto, *J. geophys. Res.* **97,** 14,761–14,772, 1992.

Tishkovets, V. P. and Shkuratov, Yu. G., Aggregates of electromagnetically interacting particles exhibit the negative polarization and opposition spike, *Bull. Amer. Astron. Soc.* **24,** 959, 1992.

Tsang, L., Ding, K. H. and Wen, B., Polarimetric signatures of random discrete scatterers based on vector radiative transfer theory, in *Progress in Electromagnetic Research* 3 (edited by J. A. Kong), pp. 75–142, Elsevier, New York, 1990.

Tsang, L., Kong, J. A. and Shin, R. T., *Theory of Microwave Remote Sensing*, Wiley, New York, 1985.

van Albada, M. P. and Lagendijk, A., Observation of weak localization of light in a random medium, *Phys. Rev. Lett.* **55,** 2692–2695, 1985.

van Albada, M. P., van der Mark, M. B. and Lagendijk, A., Polarization effects in weak localization of light, *J. Phys. D* **21,** S28–S31, 1988.

van der Mark, M. B., van Albada, M. P. and Lagendijk, A., Light scattering in strongly scattering media: multiple scattering and weak localization, *Phys. Rev. B* **37,** 3575–3592, 1988.

Wauben, W. M. F. and Hovenier, J. W., Polarized radiation of an atmosphere containing randomly-oriented spheroids, *J. Quant. Spectrosc. Radiat. Transfer* **47,** 491–504, 1992.

Wolf, P. E. and Maret, G., Weak localization and coherent backscattering of photons in disordered media, *Phys. Rev. Lett.* **55,** 2696–2699, 1985.

Wolf, P. E., Maret, G., Akkermans, E. and Maynard, R., Optical coherent backscattering by random media: an experimental study, *J. Phys. (Paris)* **49,** 63–75, 1988.

Zellner, B., 44 Nysa: an iron-depleted asteroid, *Astrophys. J. (Lett.)* **198,** L45–L47, 1975.

Zellner, B., Leake, M., Morrison, D. and Williams, J. G., The E asteroids and the origin of the enstatite achondrites, *Geochim. Cosmochim. Acta* **41,** 1759–1767, 1977.

Zook, H. A. and McCoy, J. E., Large scale lunar horizon glow and a high altitude lunar dust exosphere, *Geophys. Res. Lett.* **18,** 2117–2120, 1991.